Critical role of soluble amyloid-β for early hippocampal hyperactivity in a mouse model of Alzheimer's disease

Marc Aurel Busche[a,b,c], Xiaowei Chen[a,c], Horst A. Henning[a,c], Julia Reichwald[d], Matthias Staufenbiel[d], Bert Sakmann[a,1], and Arthur Konnerth[a,c,1]

[a]Institut für Neurowissenschaften, Technische Universität München, 80802 Munich, Germany; [b]Klinik und Poliklinik für Psychiatrie und Psychotherapie, Technische Universität München, 81675 Munich, Germany; [c]Center for Integrated Protein Science, 81377 Munich, Germany; and [d]Novartis Institutes for Biomedical Research, 4002 Basel, Switzerland

Contributed by Bert Sakmann, April 18, 2012 (sent for review January 26, 2012)

Alzheimer's disease (AD) is characterized by a progressive dysfunction of central neurons. Recent experimental evidence indicates that in the cortex, in addition to the silencing of a fraction of neurons, other neurons are hyperactive in amyloid-β (Aβ) plaque-enriched regions. However, it has remained unknown what comes first, neuronal silencing or hyperactivity, and what mechanisms might underlie the primary neuronal dysfunction. Here we examine the activity patterns of hippocampal CA1 neurons in a mouse model of AD in vivo using two-photon Ca^{2+} imaging. We found that neuronal activity in the plaque-bearing CA1 region of older mice is profoundly altered. There was a marked increase in the fractions of both silent and hyperactive neurons, as previously also found in the cortex. Remarkably, in the hippocampus of young mice, we observed a selective increase in hyperactive neurons already before the formation of plaques, suggesting that soluble species of Aβ may underlie this impairment. Indeed, we found that acute treatment with the γ-secretase inhibitor LY-411575 reduces soluble Aβ levels and rescues the neuronal dysfunction. Furthermore, we demonstrate that direct application of soluble Aβ can induce neuronal hyperactivity in wild-type mice. Thus, our study identifies hippocampal hyperactivity as a very early functional impairment in AD transgenic mice and provides direct evidence that soluble Aβ is crucial for hippocampal hyperactivity.

brain disease | in vivo imaging

Alzheimer's disease (AD) is associated with multiple neuronal dysfunctions, including impairments underlying the storage and processing of information in the brain (1). One of the major functional defects in AD is a massive decrease in neuronal activity (2, 3). This generalized silencing of brain circuits generated the synaptic failure hypothesis (4). Interestingly, more recent studies revealed a more complex picture of the neuronal defects in AD, demonstrating a mix of both hypoactivity and hyperactivity in various brain regions. For example, in transgenic mice overexpressing both mutant human amyloid precursor protein (APP) and mutant human presenilin 1 (PS1), half of the neurons in layer 2/3 of the cortex were functionally impaired, with a decrease in neuronal activity in 29% of the neurons (termed "silent" neurons) and a profound increase in more than 20% of neurons (termed "hyperactive" neurons) (5). Interestingly, the increase in hyperactive neurons was most prominent in the vicinity of plaques. Such alterations of cortical activity were not observed in predepositing transgenic mice or in wild-type mice, indicating that the changes in neuronal activity were temporally correlated with the histological pathology. Consistently, resting Ca^{2+} levels in cortical dendrites of APP/PS1 transgenic mice were substantially increased in the area surrounding plaques (6). Furthermore, APP transgenic mice exhibited nonconvulsive seizure activity in cortex and hippocampus, which was associated with GABAergic sprouting, enhanced synaptic inhibition, and synaptic plasticity defects (7). Thus, synaptic depression and excess neuronal activity appear to coexist in an unknown manner in AD; however, it is entirely unclear what comes first, neuronal silencing or hyperactivity, and whether plaques are directly involved in the initiation of neuronal dysfunction.

The hippocampal CA1 pyramidal cell circuit represents a particularly good model system to address this question, because the hippocampus is known to be a very early target in AD. First, impaired learning and memory, which are believed to involve hippocampal dysfunction (8), are typically among the first symptoms of the disease both in animal models and humans (9, 10). Second, previous animal studies provided clear evidence that structural hippocampal abnormalities can occur at very early stages of the disease, well before the emergence of plaques (11–13). However, the implications of such findings for the function of hippocampal neuronal populations in vivo are unknown, mainly because the hippocampus has been inaccessible to cellular-level imaging. Inspired by the finding that the hippocampus can be exposed by suction removal of overlying cortex (14), recent reports have demonstrated that two-photon imaging of the hippocampus in vivo, allowing detailed studies with single-cell resolution, is feasible (15, 16). Here we introduce an optimized protocol for two-photon Ca^{2+} imaging of CA1 neuronal populations in AD transgenic mice in vivo and reveal the functional impairments of the hippocampal circuit in the presence and absence of plaques.

Results

For our study, we used transgenic mice overexpressing both mutated APP_{swe} and mutated $PS1_{G384A}$ in neurons. These mutations are known to induce a rapid increase in soluble brain Aβ levels, followed by the formation of plaques beginning at an age of about 3 mo (5). To analyze plaque formation in the hippocampus in more detail, we stained sections from transgenic mice with thioflavin-S and 4G8 antibody against **Aβ**. No plaques were detected in mice 1–2 mo of age, whereas many plaques were found in mice 6–7 mo of age (Fig. S1), consistent with previous observations (5).

Neuronal Silencing and Hyperactivity in the Hippocampus of Plaque-Bearing Transgenic Mice. The hippocampus is located beneath the cortex and cannot be directly visualized by two-photon microscopy. Therefore, we removed unilaterally a small (1–2 mm diameter) cortical region covering the dorsal hippocampus (14–16) and then used bulk loading (17, 18) of the fluorescent Ca^{2+} indicator Fluo-8 AM combined with two-photon microscopy to probe the spontaneous activity of neuronal populations in the CA1 pyramidal cell layer in vivo (Fig. 1 *A* and *B*). We first analyzed 6- to 7-mo-old transgenic mice that were depositing plaques and found that the pattern of hippocampal neuronal activity was significantly altered compared with age-matched wild-type mice (Fig. 1 *C* and *D*). According to a previous assessment of neurons in cortex (5),

Author contributions: M.A.B., M.S., B.S., and A.K. designed research; M.A.B., X.C., H.A.H., J.R., M.S., and A.K. performed research; M.A.B., X.C., H.A.H., J.R., M.S., and A.K. analyzed data; and M.A.B., M.S., B.S., and A.K. wrote the paper.

The authors declare no conflict of interest.

[1]To whom correspondence may be addressed. E-mail: berninger@neuro.mpg.de or arthur.konnerth@lrz.tum.de.

This article contains supporting information online at www.pnas.org/lookup/suppl/doi:10.1073/pnas.1206171109/-/DCSupplemental.

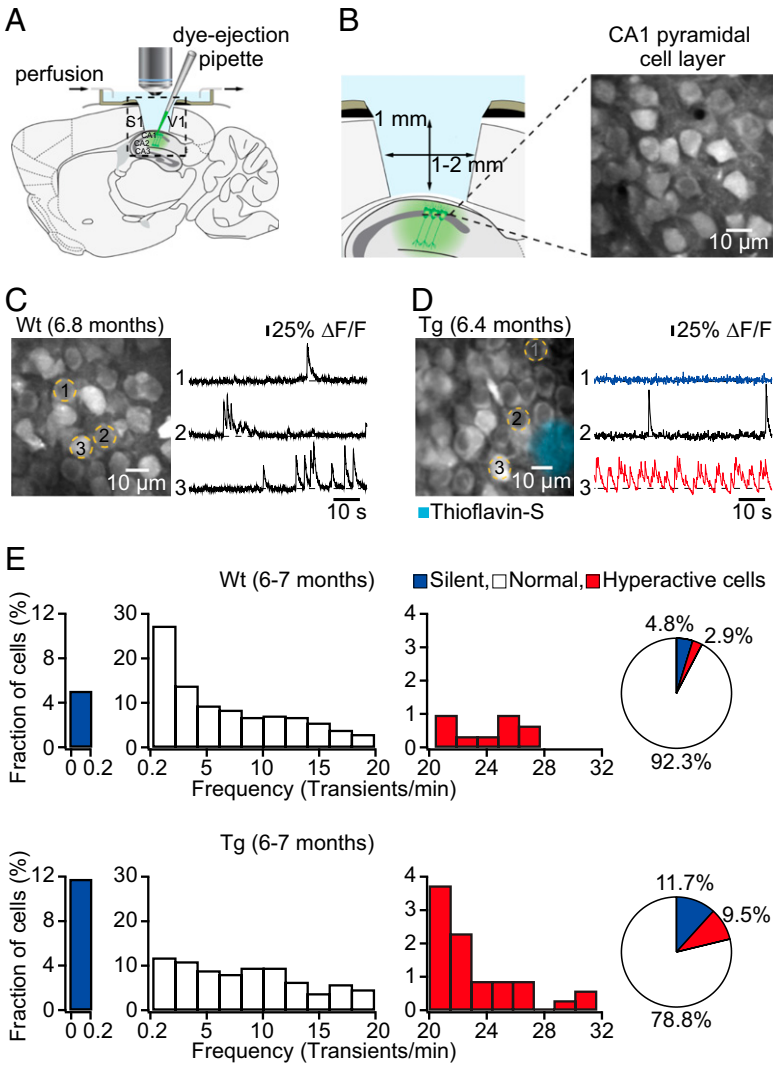

Fig. 1. Altered neuronal activity in hippocampus of plaque-bearing transgenic mice. (*A*) Schematic of the experimental preparation for in vivo imaging. (*B*) (*Left*) Detailed view of the boxed region in *A*. (*Right*) In vivo image of a CA1 pyramidal cell layer. (*C*) (*Left*) CA1 neurons imaged in vivo in a wild-type mouse. (*Right*) Spontaneous Ca^{2+} transients of the corresponding neurons marked (*Left*). (*D*) (*Left*) CA1 neurons imaged in vivo in a transgenic (tg) mouse with thioflavin-S–positive plaques (light blue). (*Right*) Spontaneous Ca^{2+} transients of the corresponding neurons marked (*Left*). Traces are color-coded to mark neurons that were either silent (blue) or hyperactive (red) during the recording period. (*E*) Histograms showing the frequency distribution of Ca^{2+} transients in wild-type (*Upper*; n = 312 cells in five mice) and tg (*Lower*; n = 349 cells in five mice) mice. Note increased fractions of silent and hyperactive neurons in tg mice. Pie charts show the relative proportions of silent, normal, and hyperactive neurons.

we classified all recorded neurons based on their individual activity rates as silent (0–0.2 transients/min), normal (0.2–20 transients/min), or hyperactive (≥20 transients/min). We found that the fraction of neurons that were silent was significantly larger in transgenic (11.72 ± 0.65%, n = 5 mice) compared with wild-type mice (4.76 ± 0.31%, n = 5 mice; $P < 0.001$, Student's t test) (Fig. 1*E*). In addition, the fraction of hyperactive neurons was significantly larger in transgenic (9.51 ± 1.75%, n = 5 mice) compared with wild-type mice (2.86 ± 0.63%, n = 5 mice; $P < 0.001$, Student's t test) (Fig. 1*E*). Also, we found that hyperactive neurons were located exclusively in the vicinity of plaques in transgenic mice, whereas both silent and normal neurons were distributed throughout the hippocampus (Fig. S2). These alterations of hippocampal activity were qualitatively identical to those previously observed in cortex (5).

Early Hyperactivity of Hippocampal Neurons in Predepositing Transgenic Mice. We next studied spontaneous neuronal activity in the CA1 pyramidal cell layer of 1- to 2-mo-old transgenic mice, an age when no plaques were detectable (Fig. S1 *A* and *C*). Surprisingly, we found that the majority of CA1 neurons in transgenic mice exhibited markedly elevated rates of spontaneous Ca^{2+} transients, compared with age-matched wild-type mice (Fig. 2 *A* and *B*). Further analyses demonstrated that the frequency distribution of spontaneous Ca^{2+} transients was generally shifted toward higher values in transgenic mice compared with wild-type mice (Fig. 2*C* and Fig. S3), resulting in a strong increase in the median frequency of Ca^{2+} transients in transgenic (12.37 transients/min, n = 818 cells in seven mice) compared with wild-type mice (4.54 transients/min, n = 693 cells in six mice; $P < 0.001$, Kolmogorov–Smirnov test). As in 6- to 7-mo-old transgenic mice, we classified all recorded neurons based on their individual activity rates as silent (0–0.2 transients/min), normal (0.2–20 transients/min), or hyperactive (≥20 transients/min) (Fig. 2*C*). We found that the fraction of hyperactive neurons was significantly larger in transgenic (25.85 ± 3.59%, n = 7 mice) compared with wild-type mice (1.85 ± 0.86%, n = 6 mice; $P < 0.001$, Student's t test) (Fig. 2*C*). Notably, there was a trend

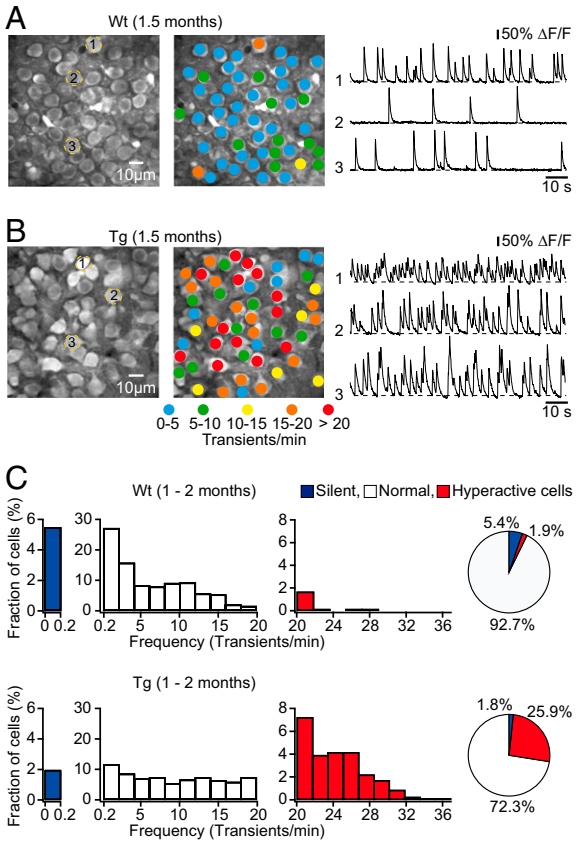

Fig. 2. Abnormal hyperactivity of hippocampal neurons in predepositing transgenic mice. (*A* and *B*) (*Left*) CA1 neurons imaged in vivo in a wild-type and a transgenic mouse, respectively. (*Center*) Activity maps, in which hue is determined by the frequency of spontaneous Ca^{2+} transients, overlaid with the anatomical image (*Left*). (*Right*) Spontaneous Ca^{2+} transients of the corresponding neurons marked (*Left*). (*C*) The frequency distribution of spontaneous Ca^{2+} transients was shifted toward higher frequencies in tg (*Lower*; n = 818 cells in seven mice) compared with wild-type mice (*Upper*; n = 693 cells in six mice). Pie charts show the relative proportions of silent, normal, and hyperactive neurons.

toward a smaller proportion of silent cells in transgenic (1.81 ± 0.57%, n = 7 mice) compared with wild-type mice (5.44 ± 1.47%, n = 6 mice; P = 0.057, Student's t test) (Fig. 2*C*), suggesting an overall increase in excitatory drive in the predepositing transgenic mice. To compare hippocampus and cortex more directly at this age, we imaged both cortical and hippocampal neuronal activity in individual transgenic mice. We first recorded spontaneous neuronal activity in layer 2/3 of the cortex and found that it was indistinguishable from that in wild-type mice (Fig. S4 *A* and *C*), consistent with previous findings (5). We then removed a small portion of the cortex in the same mouse and recorded spontaneous activity of hippocampal neurons. We found an abnormal increase in hippocampal activity compared with wild-type mice (Fig. S4 *B* and *D*), confirming our previous observation that the function of hippocampal neurons is altered long before that of cortical neurons (Fig. 2). Together, the results indicate that the earliest functional deficits of neurons and circuits occur in the hippocampus, progressing with age to the cortex.

Although it had been shown that Ca^{2+} transients in cortical neurons are evoked exclusively through synaptically mediated action potential firing (19, 20), the mechanisms underlying Ca^{2+} signaling in hippocampal neurons have remained unclear. This issue is particularly important, because several lines of evidence suggest that the intracellular Ca^{2+} homeostasis may be disturbed in AD transgenic mice (6, 21, 22). To determine the relationship between Ca^{2+} transients and the electrical cellular activity in the hippocampus, we combined cell-attached recordings with Ca^{2+} imaging. Not surprisingly, we found that neuronal Ca^{2+} transients exclusively reported the firing of action potentials in wild-type mice (Fig. 3 *A* and *B*). We reliably detected 73% of all single-action potentials and 100% of all trains of two or more action potentials in the recorded cells (Fig. 3*C*). As mentioned above, the neuronal Ca^{2+} homeostasis may be altered in transgenic mice (6, 21, 22). Thus, Ca^{2+} release from intracellular stores could contribute to Ca^{2+} signals in transgenic mice and confound our interpretation of Ca^{2+} transients as an indirect measure of action potential firing. To determine the mechanisms underlying Ca^{2+} signaling in transgenic mice, we first applied the ionotropic glutamate receptor blockers 6-cyano-7-nitroquinoxaline-2,3-dione (CNQX) and D,L-2-amino-5-phosphonovaleric acid (APV). We found that spontaneous Ca^{2+} transients were completely abolished (n = 3 mice; Fig. 3*D*), indicating that Ca^{2+} transients were exclusively evoked by synaptic activity. We then combined cell-attached recordings with Ca^{2+} imaging in transgenic mice and demonstrated that Ca^{2+} transients were exclusively triggered by action potentials (Fig. 3 *E* and *F*).

Rescue of Neuronal Hyperactivity by Acute γ-Secretase Inhibition. The observation that hyperactivity is present in the absence of plaques indicated an important role of soluble Aβ. To test this hypothesis more directly, we treated 1- to 2-mo-old transgenic mice with the γ-secretase inhibitor LY-411575, which has previously been shown to rapidly reduce soluble Aβ levels in vivo (23, 24). Indeed, we found that administration of a single oral

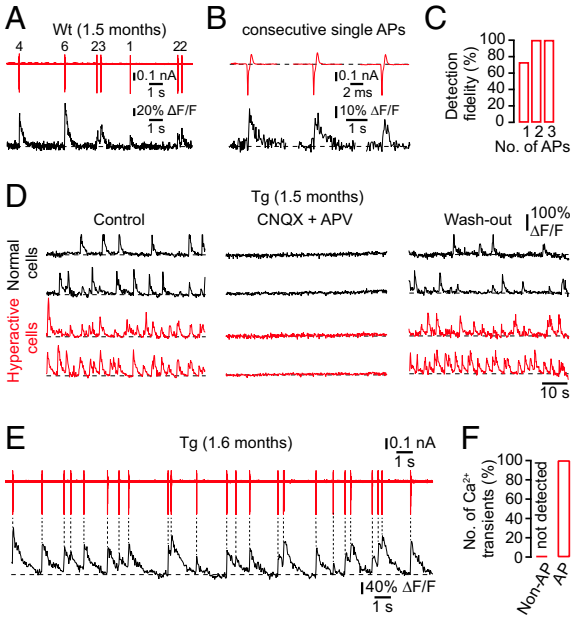

Fig. 3. Cellular mechanisms of spontaneous Ca^{2+} transients in wild-type and transgenic mice. (*A*) Simultaneous in vivo recordings of spontaneous Ca^{2+} transients (black trace) and underlying action potential (AP) firing (red trace; number of APs indicated) in a cell-attached configuration from a CA1 neuron in a wild-type mouse. (*B*) Examples of spontaneous Ca^{2+} transients (black trace) evoked from three consecutive single APs (red trace) in a WT mouse. (*C*) Fractions of single APs and trains of APs optically detected in CA1 neurons of WT mice (n = 15 cells in three mice). (*D*) Spontaneous Ca^{2+} transients in normal (black traces) and hyperactive (red traces) CA1 neurons of a transgenic mouse before, during, and after local application of CNQX and APV. (*E*) Simultaneous in vivo recordings of spontaneous Ca^{2+} transients (black trace) and underlying action potential firing (red trace) in a cell-attached configuration from a CA1 neuron in a tg mouse. (*F*) Number of spontaneous Ca^{2+} transients triggered (AP) and not triggered (non-AP) by action potential firing in tg mice (n = 13 cells in three mice).

dose of 10 mg/kg LY-411575 to transgenic mice significantly reduced hippocampal levels of aqueous-soluble [Tris-buffered saline (TBS), traditionally viewed as the soluble Aβ fraction] and detergent-soluble (SDS, traditionally viewed as aggregated and membrane-associated Aβ) Aβ-40 and Aβ-42 compared with vehicle ($P < 0.001$ for Aβ-40 and $P < 0.05$ for Aβ-42, Student's t test; Fig. 4 *A* and *B*) (see also *SI Materials and Methods*, *Quantification of Amyloid-β*). We therefore examined the effect of γ-secretase inhibition on spontaneous activity in hippocampal neurons at 4–6 h after treatment, when soluble Aβ levels were lowest (23), and found that activity levels of CA1 neurons in LY-411575–treated transgenic mice were almost completely restored to the control levels recorded in wild-type mice (Fig. 4 *C–E*). Notably, the fraction of hyperactive neurons in LY-411575–treated transgenic mice (5.13 ± 1.47%, $n = 5$ mice) was similar to that in the control wild-type mice (1.85 ± 0.86%, $n = 6$ mice; $P > 0.05$, Student's t test) (Fig. 4*F* and Fig. S5). The fractions of silent neurons were also similar in LY-411575–treated transgenic (5.29 ± 2.31%, $n = 5$ mice) and wild-type mice (5.44 ± 1.47%, $n = 6$ mice; $P > 0.05$, Student's t test) (Fig. S5). It is important to note that LY-411575 treatment had no effect on hippocampal activity levels in wild-type mice ($P > 0.05$, Kolmogorov–Smirnov test; Fig. 4*G*). These results show that acute γ-secretase inhibition not only reduces soluble Aβ levels but also effectively restores neuronal dysfunction in the hippocampus of transgenic mice, suggesting that soluble Aβ is causally related to neuronal hyperactivity.

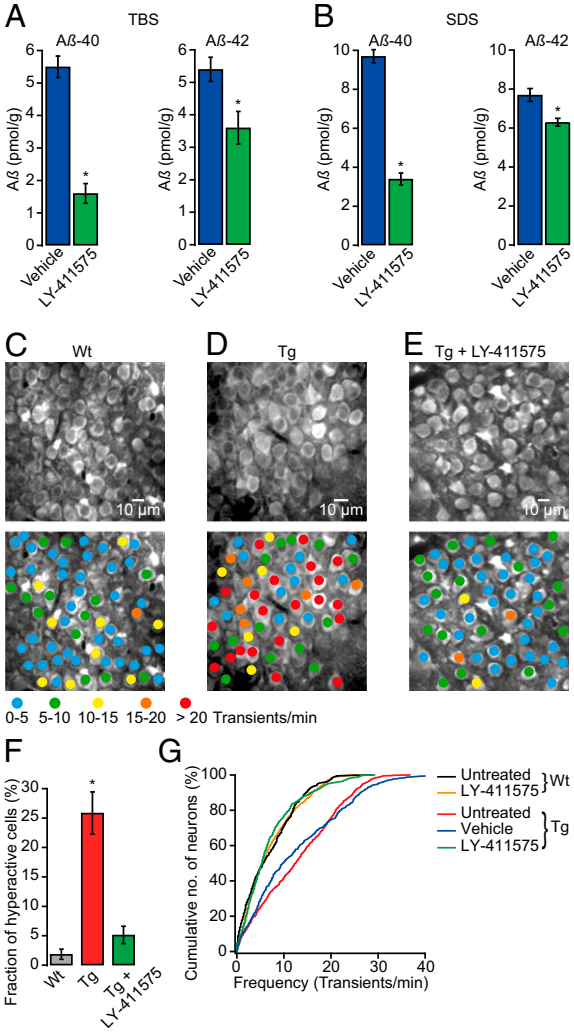

Fig. 4. A single dose of γ-secretase inhibitor reduces soluble Aβ levels and rescues neuronal dysfunction in transgenic mice. (*A* and *B*) Acute LY-411575 treatment significantly reduced TBS- and SDS-soluble Aβ-40 and Aβ-42 hippocampal levels in transgenic mice ($n = 4$–5 mice per group; $^*P < 0.001$ for Aβ-40 and $^*P < 0.05$ for Aβ-42, Student's t test). (*C–E*) (*Upper*) CA1 neurons imaged in vivo in a WT, a tg, and an LY-411575–treated tg mouse, respectively. (*Lower*) Activity maps, in which hue is determined by the frequency of spontaneous Ca^{2+} transients, overlaid with the anatomical image (*Upper*). (*F*) The fraction of hyperactive neurons was significantly smaller in LY-411575–treated tg (5.13 ± 1.47%, $n = 5$ mice) than in untreated tg mice (25.85 ± 3.59%, $n = 7$ mice; $^*P < 0.001$, Student's t test) and not significantly different from untreated WT mice (1.85 ± 0.86%, $n = 6$ mice; $P > 0.05$, Student's t test). (*G*) Cumulative distributions of spontaneous Ca^{2+} transients in LY-411575–treated tg mice ($n = 709$ cells) were not significantly different from untreated WT ($n = 693$ cells) and LY-411575–treated WT controls ($n = 841$ cells; $P > 0.05$, Kolmogorov–Smirnov test), but they were significantly different from vehicle-treated tg ($n = 484$ cells) and untreated tg mice ($n = 818$ cells; $^*P < 0.001$, Kolmogorov–Smirnov test). All error bars denote SEM.

Soluble Aβ Induces Neuronal Hyperactivity in Wild-Type Mice. The soluble fraction of Aβ includes monomers and oligomers that vary in size and shape from dimers to multimers and protofibrils (25). Converging evidence suggests that oligomers, rather than monomers, are the primary bioactive form of Aβ in AD and that dimers are not only the most abundant form of oligomer in the human brain but also the principal mediators of neurotoxicity in AD (26–30). Therefore, we used previously characterized cross-linked dimers (26, 31) to test whether they can directly mediate neuronal hyperactivity. We locally applied nanomolar concentrations of cross-linked dimers to CA1 neurons in wild-type mice while monitoring their ongoing spontaneous activity. Fig. 5*A* shows an experiment demonstrating an excitatory effect of dimers on CA1 neurons in vivo. The dimers immediately elevated the rate of Ca^{2+} transients in CA1 neurons (Fig. 5 *A–D*), indicating increased action potential firing. As a control, heat-denatured dimers

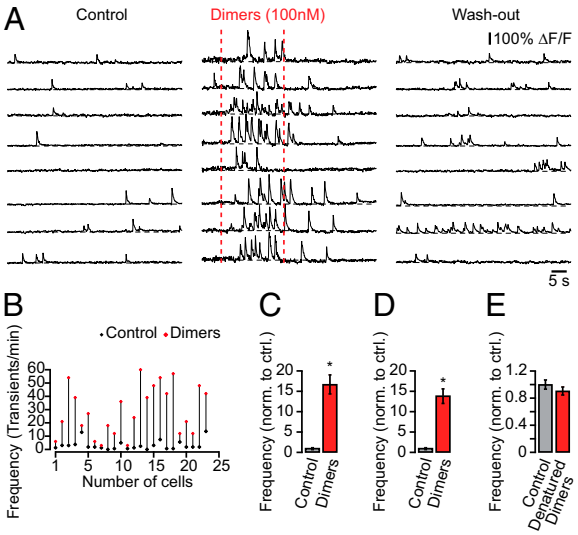

Fig. 5. Soluble Aβ induces hyperactivity in hippocampal neurons of wild-type mice. (*A*) Ca^{2+} transients in CA1 neurons of a wild-type mouse before, during, and after local application of synthetic AβS26C dimer solution (30 s, 100 nM in the application pipette). (*B*) Rates of Ca^{2+} transients in all recorded neurons from the experiment in *A* before (black) and during (red) dimer application. (*C*) Summary graph from the experiment in *A* showing the effect of dimers on the frequency of Ca^{2+} transients (normalized to control, $n = 24$ cells; $^*P < 0.001$, Student's t test). (*D*) Summary graph from all experiments illustrating the effect of dimers on the frequency of Ca^{2+} transients (normalized to control, $n = 83$ cells in three mice; $^*P < 0.001$, Student's t test). (*E*) Summary graph showing that heat-denatured dimers have no significant effect on the frequency of Ca^{2+} transients (normalized to control, $n = 158$ cells in three mice; $P > 0.05$, Student's t test). All error bars denote SEM.

NEUROSCIENCE

(dimers were boiled for 15 min, cooled to room temperature, and then locally applied) did not alter neuronal activity ($n = 158$ cells in three mice; Fig. 5*E*). In addition, the local application of the peptide vehicle (0.001% DMSO in artificial cerebrospinal fluid) alone did not alter neuronal activity ($n = 60$ neurons in two mice). These results support and extend previous in vitro observations that soluble Aβ can acutely induce inward currents in hippocampal neurons, leading to increased action potential firing and intracellular Ca^{2+} elevations (32–35). They provide further evidence that soluble Aβ can directly induce neuronal hyperactivity, which underlies early hippocampal dysfunction in transgenic mice.

Discussion

In this study, we have used two-photon microscopy to monitor the activity of neuronal populations in the hippocampal CA1 region of AD transgenic mice in vivo. Our results demonstrate that hippocampal activity was significantly altered in transgenic mice that were depositing plaques compared with wild-type mice (Fig. S6). Specifically, the fractions of neurons that were silent and hyperactive increased significantly in transgenic mice, and hyperactive neurons were preferentially found near plaques, consistent with previous findings from cortex (5). Remarkably, our experiments reveal that there was a marked increase in hippocampal activity with an excess of hyperactive neurons already before transgenic mice began to deposit plaques. We provide experimental evidence that hyperactivity is causally related to the action of soluble Aβ. First, we demonstrate that a single dose of a γ-secretase inhibitor rapidly reduced soluble Aβ levels and completely reversed neuronal hyperactivity. Second, we show that local application of soluble Aβ directly induced hyperactivity in wild-type mice. Thus, our results indicate that hippocampal neurons are abnormally hyperactive very early in the disease process and that hyperactivity is directly promoted by soluble Aβ.

A key finding of our study is that hippocampal neurons become hyperactive very early in transgenic mice, independent of plaque deposition, and that the silencing of neurons emerges only later in the disease course. This was unexpected, because in cortex, hyperactivity is temporally correlated with the formation of plaques (5). Possible explanations for this discrepancy between cortex and hippocampus (see also Fig. S7) may involve different local concentrations of soluble Aβ, different vulnerabilities for cortical and hippocampal neurons, or a combination of these features. The downstream cellular targets that are involved in Aβ-induced neuronal hyperactivity are not entirely clear yet, but may involve elevated levels of synaptic glutamate due to reductions in synaptic glutamate uptake, as previously shown in hippocampal slices treated with Aβ dimers (30). In humans with AD, there is also evidence for early functional magnetic resonance (fMRI) hyperactivation of the hippocampus, which is followed by hypoactivity at later disease stages (36, 37). However, the underlying neural basis of early fMRI hyperactivation has remained unknown. Our data now suggest that increased fMRI signal levels might be related to excessive neuronal activity, which is due to a direct action of soluble Aβ.

An important question is how alterations of neuronal activity are linked to behavioral and cognitive symptoms in AD. In animal models of AD, there is evidence that learning and memory deficits can occur before the formation of plaques, the occurrence of structural abnormalities, and neurodegeneration (4), suggesting that behavioral deficits are primarily a reflection of functional alterations of neuronal populations. Several lines of evidence have converged to support the idea that soluble Aβ peptides disrupt memory function, but the underlying neural basis has remained unclear (26, 28, 38–42). Our finding that soluble Aβ can induce hyperactivity raises the intriguing possibility that hyperactivity may be directly related to learning and memory deficits. Further experimental support for this hypothesis comes from the finding that the therapeutic effect of γ-secretase inhibition on memory deficits is similarly rapid as that on neuronal hyperactivity in AD transgenic mice (43). In addition, cerebroventricular injections of soluble Aβ rapidly and transiently induce memory deficits in wild-type mice (44), perhaps by causing transient neuronal hyperactivity.

In conclusion, our study reveals the functional impairments of neuronal populations in the hippocampus of AD transgenic mice in vivo and identifies a causal relationship between soluble Aβ and neuronal hyperactivity. Our findings not only have profound implications for the understanding of AD pathogenesis but may also provide a conceptual basis for novel pharmacological treatments directed at altered neuronal activity.

Materials and Methods

Animals and Surgery. All experimental procedures were in compliance with institutional animal welfare guidelines and were approved by the state government of Bavaria, Germany. The previously described APP23xPS45 double transgenic mouse model was used in all experiments in this paper (5). Animal preparation procedures were similar to those previously described (5, 17, 18), except for the removal of cortical tissue to expose the hippocampal surface. A detailed description is found in *SI Materials and Methods*.

Imaging. In vivo two-photon recordings were made using a custom-built two-photon microscope based on a Ti:sapphire excitation laser operating at 925 nm and a resonant galvo-mirror system (8 kHz; GSI) for *x-y* scanning (45). The laser intensity was modulated with a Pockel's cell. The laser-scanning unit was mounted on an upright microscope equipped with a water-immersion objective (Nikon; 40×, 0.8 N.A.), and fluorescence was detected using a GaAsP photomultiplier tube (H7422-40; Hamamatsu). Full-frame images were acquired at 30 Hz using custom-written software based on LabVIEW (National Instruments). At each focal plane, spontaneous Ca^{2+} transients of CA1 neurons were recorded for at least 5 min. For simultaneous visualization of Fluo-8 AM–labeled neurons and thioflavin-S–labeled plaques, the emitted fluorescence was split at 515 nm.

Image Analysis. Image analysis was performed off-line using ImageJ (National Institutes of Health) and Igor Pro (Wavemetrics). First, regions of interest (ROIs) were drawn around individual somata, and then relative fluorescence change (ΔF/F) versus time traces were generated for each ROI. Ca^{2+} transients were identified as changes in ΔF/F that were three times larger than the SD of the noise band. Astrocytes were excluded from the analysis based on their selective staining by sulforhodamine 101 (46) and their specific morphology.

Cell-Attached Recordings. Somatic cell-attached recordings of Fluo-8 AM–labeled CA1 neurons were obtained using an EPC10 amplifier (USB Quadro Amplifier; HEKA Elektronik) by the "shadow-patching" procedure (47) under two-photon imaging guidance. The patch pipette solution contained artificial cerebrospinal fluid (ACSF) with 50 μM Alexa Fluor 594 (Invitrogen) for pipette visualization. The pipettes had resistances of 5–7 MΩ. Electrophysiological data were filtered at 10 kHz and sampled at 20 kHz using Patchmaster software (HEKA Elektronik).

Treatment with LY-411575. The γ-secretase inhibitor LY-411575 (23, 24) was suspended in 0.5% methylcellulose at a concentration of 10 mg/kg. Mice received a single dose of inhibitor by oral gavage at 10 mg/kg. Control animals received a single dose of vehicle (0.5% methylcellulose in water) instead of γ-secretase inhibitor treatment.

Dimer Application. Synthetic $Aβ_{40}S26C$ dimers (26, 27, 31) were purchased from Anaspec and dissolved in DMSO. This dimer preparation was diluted to 100 nM in ACSF, filled into a micropipette, and locally pressure-applied to the cells of interest (30 s, 0.15 bar).

Quantification of Aβ and Detection of Plaques. A detailed description is in *SI Materials and Methods*.

Statistical Analysis. Statistical analysis was performed using SPSS (SPSS). The statistical methods used were the Student's *t* test and the Kolmogorov–Smirnov test. $P < 0.05$ was considered statistically significant.

ACKNOWLEDGMENTS. We thank Jia Lou for excellent technical assistance. This work was supported by the Deutsche Forschungsgemeinschaft (IRTG 1373), the European Research Area-Net Program, and the Schiedel Foundation. A.K. is a Carl-von-Linde Senior Fellow of the Institute for Advanced Study of the Technische Universität München.

1. Mattson MP (2004) Pathways towards and away from Alzheimer's disease. *Nature* 430:631–639.
2. Silverman DH, et al. (2001) Positron emission tomography in evaluation of dementia: Regional brain metabolism and long-term outcome. *JAMA* 286:2120–2127.
3. Prvulovic D, Van de Ven V, Sack AT, Maurer K, Linden DE (2005) Functional activation imaging in aging and dementia. *Psychiatry Res* 140(2):97–113.
4. Selkoe DJ (2002) Alzheimer's disease is a synaptic failure. *Science* 298:789–791.
5. Busche MA, et al. (2008) Clusters of hyperactive neurons near amyloid plaques in a mouse model of Alzheimer's disease. *Science* 321:1686–1689.
6. Kuchibhotla KV, et al. (2008) Aβ plaques lead to aberrant regulation of calcium homeostasis in vivo resulting in structural and functional disruption of neuronal networks. *Neuron* 59:214–225.
7. Palop JJ, et al. (2007) Aberrant excitatory neuronal activity and compensatory remodeling of inhibitory hippocampal circuits in mouse models of Alzheimer's disease. *Neuron* 55:697–711.
8. Squire LR, Zola-Morgan S (1991) The medial temporal lobe memory system. *Science* 253:1380–1386.
9. Hyman BT, Van Hoesen GW, Damasio AR, Barnes CL (1984) Alzheimer's disease: Cell-specific pathology isolates the hippocampal formation. *Science* 225:1168–1170.
10. Moran PM, Higgins LS, Cordell B, Moser PC (1995) Age-related learning deficits in transgenic mice expressing the 751-amino acid isoform of human β-amyloid precursor protein. *Proc Natl Acad Sci USA* 92:5341–5345.
11. Mucke L, et al. (2000) High-level neuronal expression of $A\beta_{1-42}$ in wild-type human amyloid protein precursor transgenic mice: Synaptotoxicity without plaque formation. *J Neurosci* 20:4050–4058.
12. Hsia AY, et al. (1999) Plaque-independent disruption of neural circuits in Alzheimer's disease mouse models. *Proc Natl Acad Sci USA* 96:3228–3233.
13. Moechars D, et al. (1999) Early phenotypic changes in transgenic mice that overexpress different mutants of amyloid precursor protein in brain. *J Biol Chem* 274: 6483–6492.
14. Kandel ER, Spencer WA, Brinley FJ, Jr. (1961) Electrophysiology of hippocampal neurons. I. Sequential invasion and synaptic organization. *J Neurophysiol* 24:225–242.
15. Dombeck DA, Harvey CD, Tian L, Looger LL, Tank DW (2010) Functional imaging of hippocampal place cells at cellular resolution during virtual navigation. *Nat Neurosci* 13:1433–1440.
16. Mizrahi A, Crowley JC, Shtoyerman E, Katz LC (2004) High-resolution in vivo imaging of hippocampal dendrites and spines. *J Neurosci* 24:3147–3151.
17. Stosiek C, Garaschuk O, Holthoff K, Konnerth A (2003) In vivo two-photon calcium imaging of neuronal networks. *Proc Natl Acad Sci USA* 100:7319–7324.
18. Garaschuk O, Milos RI, Konnerth A (2006) Targeted bulk-loading of fluorescent indicators for two-photon brain imaging in vivo. *Nat Protoc* 1:380–386.
19. Rochefort NL, et al. (2009) Sparsification of neuronal activity in the visual cortex at eye-opening. *Proc Natl Acad Sci USA* 106:15049–15054.
20. Kerr JN, Greenberg D, Helmchen F (2005) Imaging input and output of neocortical networks in vivo. *Proc Natl Acad Sci USA* 102:14063–14068.
21. Bezprozvanny I, Mattson MP (2008) Neuronal calcium mishandling and the pathogenesis of Alzheimer's disease. *Trends Neurosci* 31:454–463.
22. Goussakov I, Miller MB, Stutzmann GE (2010) NMDA-mediated Ca^{2+} influx drives aberrant ryanodine receptor activation in dendrites of young Alzheimer's disease mice. *J Neurosci* 30:12128–12137.
23. Abramowski D, et al. (2008) Dynamics of Aβ turnover and deposition in different β-amyloid precursor protein transgenic mouse models following γ-secretase inhibition. *J Pharmacol Exp Ther* 327:411–424.
24. Lanz TA, Hosley JD, Adams WJ, Merchant KM (2004) Studies of Aβ pharmacodynamics in the brain, cerebrospinal fluid, and plasma in young (plaque-free) Tg2576 mice using the γ-secretase inhibitor N2-[(2S)-2-(3,5-difluorophenyl)-2-hydroxyethanoyl]-N1-[(7S)-5-methyl-6-oxo-6,7-dihydro-5H-dibenzo[b,d]azepin-7-yl]-L-alaninamide (LY-411575). *J Pharmacol Exp Ther* 309(1):49–55.
25. Haass C (2010) Initiation and propagation of neurodegeneration. *Nat Med* 16: 1201–1204.
26. Shankar GM, et al. (2008) Amyloid-β protein dimers isolated directly from Alzheimer's brains impair synaptic plasticity and memory. *Nat Med* 14:837–842.
27. Hu NW, Smith IM, Walsh DM, Rowan MJ (2008) Soluble amyloid-β peptides potently disrupt hippocampal synaptic plasticity in the absence of cerebrovascular dysfunction in vivo. *Brain* 131:2414–2424.
28. Mc Donald JM, et al.; Medical Research Council Cognitive Function and Ageing Study (2010) The presence of sodium dodecyl sulphate-stable Aβ dimers is strongly associated with Alzheimer-type dementia. *Brain* 133:1328–1341.
29. Li S, Shankar GM, Selkoe DJ (2010) How do soluble oligomers of amyloid β-protein impair hippocampal synaptic plasticity? *Front Cell Neurosci* 4:5.
30. Li S, et al. (2009) Soluble oligomers of amyloid β protein facilitate hippocampal long-term depression by disrupting neuronal glutamate uptake. *Neuron* 62:788–801.
31. O'Nuallain B, et al. (2010) Amyloid β-protein dimers rapidly form stable synaptotoxic protofibrils. *J Neurosci* 30:14411–14419.
32. Brorson JR, et al. (1995) The Ca^{2+} influx induced by β-amyloid peptide 25–35 in cultured hippocampal neurons results from network excitation. *J Neurobiol* 26:325–338.
33. Sanchez-Mejia RO, et al. (2008) Phospholipase A2 reduction ameliorates cognitive deficits in a mouse model of Alzheimer's disease. *Nat Neurosci* 11:1311–1318.
34. Snyder EM, et al. (2005) Regulation of NMDA receptor trafficking by amyloid-β. *Nat Neurosci* 8:1051–1058.
35. Alberdi E, et al. (2010) Amyloid β oligomers induce Ca^{2+} dysregulation and neuronal death through activation of ionotropic glutamate receptors. *Cell Calcium* 47:264–272.
36. O'Brien JL, et al. (2010) Longitudinal fMRI in elderly reveals loss of hippocampal activation with clinical decline. *Neurology* 74:1969–1976.
37. Dickerson BC, et al. (2005) Increased hippocampal activation in mild cognitive impairment compared to normal aging and AD. *Neurology* 65:404–411.
38. Walsh DM, et al. (2002) Naturally secreted oligomers of amyloid β protein potently inhibit hippocampal long-term potentiation in vivo. *Nature* 416:535–539.
39. Cheng IH, et al. (2007) Accelerating amyloid-β fibrillization reduces oligomer levels and functional deficits in Alzheimer disease mouse models. *J Biol Chem* 282: 23818–23828.
40. Tomiyama T, et al. (2010) A mouse model of amyloid β oligomers: Their contribution to synaptic alteration, abnormal tau phosphorylation, glial activation, and neuronal loss in vivo. *J Neurosci* 30:4845–4856.
41. Cleary JP, et al. (2005) Natural oligomers of the amyloid-β protein specifically disrupt cognitive function. *Nat Neurosci* 8(1):79–84.
42. Lesné S, et al. (2006) A specific amyloid-β protein assembly in the brain impairs memory. *Nature* 440:352–357.
43. Comery TA, et al. (2005) Acute γ-secretase inhibition improves contextual fear conditioning in the Tg2576 mouse model of Alzheimer's disease. *J Neurosci* 25: 8898–8902.
44. Balducci C, et al. (2010) Synthetic amyloid-β oligomers impair long-term memory independently of cellular prion protein. *Proc Natl Acad Sci USA* 107:2295–2300.
45. Sanderson MJ, Parker I (2003) Video-rate confocal microscopy. *Methods Enzymol* 360: 447–481.
46. Nimmerjahn A, Kirchhoff F, Kerr JN, Helmchen F (2004) Sulforhodamine 101 as a specific marker of astroglia in the neocortex in vivo. *Nat Methods* 1(1):31–37.
47. Kitamura K, Judkewitz B, Kano M, Denk W, Häusser M (2008) Targeted patch-clamp recordings and single-cell electroporation of unlabeled neurons in vivo. *Nat Methods* 5(1):61–67.